Higher-Order Effects in Boundary-Layer Premixed Combustion

C. Treviño,* W. Stüttgen,† and N. Peters‡
Institut für Technishe Mechanik, Aachen, Federal Republic of Germany

Higher-order effects in the boundary-layer theory are included in the present analysis to evaluate the interaction of the expansion process from the premixed combustion of reacting gases with the potential flow. Two cases are considered: 1) the premixed combustion process, which takes place above the flat plate, and 2) the premixed flame, which is generated in the wake of the flat plate. In both cases, the strong expansion process, when interacting with the outer inviscid flow, produces relatively strong pressure gradients, modifying the aerodynamic structure of the flow.

Nomenclature

f = nondimensional stream function, $= \psi^*/(2x^*\rho_\infty^*\mu_\infty^* u_\infty^*)^{1/2}$
Pr = Prandtl number
p = nondimensional pressure, $= (p^* - p_\infty^*)/(\rho_\infty^* u_\infty^{*2})$
Q = nondimensional heat of reaction, $= Q^*/c_p T_\infty^*$
Q^* = heat of reaction per unit mass of fuel consumed
Re = Reynolds number, $= u_\infty^* \rho_\infty^* L^*/\mu_\infty^*$
Sc_α = Schmidt number of species α
T^* = temperature
T_α^* = activation temperature
u_∞ = freestream velocity
V = nondimensional transversal velocity, $= (\mu_\infty^*\rho_\infty^* u_\infty^*/L^*)^{-1/2} v^*$
W_α = molecular weight of species α
x^* = longitudinal coordinate
Y_F = mass concentration of the fuel (mass of fuel/total mass of mixture)
y_F = reduced mass concentration of fuel, $= Y_F/Y_{F\infty}$
y_q = quenching distance
y^* = transversal coordinate
ζ = nondimensional axial coordinate, $= (A^* Y_F^2 \nu_0 x^*)/(W_F u_\infty^*)$
η = nondimensional coordinate, $= (2\rho_\infty^*\mu_\infty^* x^*/u_\infty^*)^{-1/2}\int_0^{y^*}\rho^*\,dy^*$
θ = nondimensional temperature, $= T^*/T_\infty^*$
μ = dynamic viscosity
ρ = gas density

Subscripts

L = trailing edge of the plate
w = plate
∞ = freestream
0 = zeroth-order solution
1 = first-order solution

Superscripts

$-$ = outer potential flow region
$*$ = physical units

Introduction

FLAMES in boundary-layer flows have been studied in the past, particularly relating to flame stabilization in premixed gases and flame spread over condensed fuels. In most of the analyses it has been assumed that the leading boundary-layer equation (Prandtl boundary-layer approximation) is applicable. Regarding premixed flames, there are two different stabilization mechanisms.[1,2] In the continuous ignition mechanism, the energy for ignition is provided by the heat flux from the heated plate to the gaseous mixture and not from the flame generated downstream. In this case, the longitudinal heat and mass diffusion do not play an important role, and the Prandtl boundary-layer approximation is valid. The system of differential equations then becomes parabolic in the longitudinal direction. This type of stabilization mechanism occurs when the fluid velocity is much larger than the burning velocity of the mixture. If we assume that the flame velocity is zero or very small for values of the transverse coordinate y less than a critical distance (quenching distance y_q) and almost constant for values of $y > y_q$, then the critical velocity ratio has to be obtained at $y = y_q$ at the flame leading edge. However, if both velocities are of the same order of magnitude, the flame perturbs the flowfield in front of it making it possible to propagate upstream and reach the equilibrium position, where the flame velocity equals the fluid velocity at the quenching distance. This second type of stabilization mechanism is called the equilibrium mechanism. In this case, the Prandtl boundary-layer approximation is no longer valid, and the governing equations are the full Navier-Stokes equations, together with the energy and species concentration equations. In this case, there is a complicated feedback mechanism supporting the flame at that position.

There is experimental evidence that premixed flames are stabilized by aerodynamic effects such as low local velocities and even flow recirculation that would not exist without the presence of the flame.[3] These recirculating flows are generated by pressure gradients that are induced by the interaction of the flame with the inviscid flow, producing the separation of the boundary layer. In diffusion flame experiments in boundary-layer with injection,[4] pressure gradients have been predicted from the measured velocity field in the vicinity of the flame leading edge. The existence of low- and high-pressure regions suggests the possibility of using higher-order effects in the boundary-layer approximation that influence the structure and show the interactions between the flame and the flowfield.

Higher-order effects in reacting and nonreacting boundary-layer flows are very important for predicting boundary-layer separation and correcting drag coefficients of bodies in moderate-Reynolds-number flows.[5-8] In particular, higher-order effects are very important in processes with density variations. In this case, the expansion of the gas flowing along the body changes the displacement thickness in an important way, producing a strong interaction with the potential flow. Few works on this subject have been reported in the literature.[9] Higher-order effects in combustion processes were considered in several works.[10,11] Treviño and Fernández-Pello[10] considered higher-order effects including the longitudinal diffusion

Received June 17, 1988; revision received Oct. 14, 1988.

*Currently, Faculty of Engineering, UNAM, Mexico.
†Graduate Student.
‡Institute Head.

terms. They obtained a pressure pattern similar to that deduced for laminar diffusion flames.[4] The free interaction with the outer potential flow was not considered.

This paper shows how the Prandtl boundary-layer approximation breaks down as the flow Reynolds number decreases. The first of the higher-order effects is represented by the interaction with the external inviscid flow. The objective of the present work is to study this interaction using higher-order effects in the combustion process in a boundary-layer flow.

Problem Definition

The physical model analyzed consists of the following: A cold combustible mixture flows over a heated plate that has a uniform temperature. Two types of boundary conditions can be addressed. The first one corresponds to an infinite plate. Here the flame is formed above the flat plate. In the second one, the plate ends before a premixed flame can be formed above it. The flame then develops in the wake of the flat plate and is associated with very strong expansion effects. Using the zeroth-order boundary-layer analysis, which represents a set of parabolic differential equations in the longitudinal direction, it is not possible to obtain any feedback mechanism that reproduces the main features of this combustion process as the Reynolds number decreases. The main features of this feedback mechanism can be obtained by using higher-order approximations in the boundary-layer flow. The first-order analysis takes into account the free interaction between the boundary layer and the potential flow far away from the surface. It considers the displacement of this outer potential flow by the boundary layer. Because the governing equations in the potential flow are elliptic, this interaction produces a feedback mechanism through the generation of pressure gradients.

Here for simplicity we consider a global irreversible gas-phase chemical reaction of the Arrhenius type given by

$$w^* = A^* c_F^* c_O^* \exp(-E^*/R^*T^*) \tag{1}$$

where w^* is the net consumption rate of fuel in mass per unit times unit volume; A^* the pre-exponential factor; c_α^* the molar concentration of the reactant α per unit volume; E^* the overall activation energy of the chemical reaction; R^* the universal gas constant; and T^* the temperature of the mixture. The assumed overall chemical reaction can be written as

$$\{F\} + \nu_0\{O\} \Rightarrow \nu_p\{P\} \tag{2}$$

where ν_α corresponds to the stoichiometric coefficients of species α in the chemical reaction. The species F, O, and P represent the fuel, oxidant, and product, respectively. The nondimensional boundary-layer equations, valid up to terms of order $R^{-1/2}$, where R is the Reynolds number based on the length of the plate, are given by[11]

$$\mathfrak{L}(1,\ \partial f/\partial\eta) = 2\theta\zeta\ \partial p/\partial\eta \tag{3}$$

$$\mathfrak{L}(Pr,\theta) = -2Q\zeta y_F^2 \exp(-\theta_a/\theta) \tag{4}$$

$$\mathfrak{L}(Sc_F, y_F) = 2Q\zeta y_F^2 \exp(-\theta_a/\theta) \tag{5}$$

where $\mathfrak{L}$ denotes a differential operator defined by

$$\mathfrak{L}(m,t) = 1/m\ \partial^2 t/\partial\eta^2 + f\partial t/\partial\eta - 2\zeta(\partial f/\partial\eta\ \partial t/\partial\zeta - \partial f/\partial\zeta\ \partial t/\partial\eta) \tag{6}$$

The nondimensional boundary conditions are given by

$$\text{at}\quad \eta = 0,\ \zeta < \zeta_L;\qquad f = \partial f/\partial\eta = \theta_w = \partial y_F/\partial\eta = 0$$

$$\zeta > \zeta_L;\qquad f = \partial^2 f/\partial\eta^2 = \partial\theta/\partial\eta = \partial y_F/\partial\eta = 0 \tag{7}$$

For $\eta\to\infty$, the solution must match with the outer potential flow. The outer equations, up to terms of order $R^{-1/2}$, correspond to the classical incompressible Euler equations. Therefore, the nondimensional outer equations take the form

$$\nabla^2\bar\psi = \partial^2\bar\psi/\partial\zeta^2 + \partial^2\bar\psi/\partial\xi^2 = 0 \tag{8}$$

where

$$\bar\psi = (A^*L^*Y_F^{*2}\nu_0\psi^*)/(u^{*2}W_F)$$

$$(\zeta,\xi) = A^*L^*Y_F^2\nu_0(u^*W_F)^{-1}(x^*,y^*)$$

where ψ^* represents the stream function defined by $u^* = \partial\psi^*/\partial y^*$ and $v^* = -\partial\psi^*/\partial x^*$. The boundary conditions are given by

$$\text{at}\quad \xi\to\infty,\qquad \zeta\to-\infty,\qquad \partial\bar\psi/\partial\xi = 1$$

together with the matching conditions with the boundary-layer flow. Because the boundary layer displaces the outer flow proportional to $R^{-1/2}$, the following expansions are assumed:

$$\Omega = \Omega_0 + R^{-1/2}\Omega_1 + O(R^{-1}) \tag{9}$$

both in the boundary-layer and in the outer potential flow, where Ω represents any of the variables involved in the process. In the outer inviscid flow, the equations are then given by

$$\nabla^2\bar\psi_0 = \nabla^2\bar\psi_1 = 0 \tag{10}$$

with the nondimensional boundary conditions given by

$$\text{at}\quad \xi\to\infty,\qquad \zeta\to-\infty,\qquad \partial\bar\psi_0/\partial\xi = 1$$

$$\text{and}\qquad \partial\bar\psi_1/\partial\xi = 0$$

To the zeroth order, matching with the boundary layer requires in the asymptotic limit $\xi\to0$, $\eta\to\infty$,

$$(\partial\bar\psi_0/\partial\xi)_{\xi\to0} = (\partial f_0/\partial\eta)_{\eta\to\infty} \tag{11}$$

This is satisfied automatically, and the solution to the zeroth order corresponds to the parallel flow:

$$\bar\psi_0 = \xi \qquad\text{and}\qquad p_0 = 0 \tag{12}$$

The solution to the first-order outer equations can be found using the linearized thin airfoil theory,[12] obtaining the following integral relationship between both components of velocity at the edge of the boundary layer:

$$\bar u_1(\zeta,0) = 1/\pi\ P\!\!\int_0^\infty \frac{\bar v_1(\zeta',0)\ d\zeta'}{\zeta-\zeta'} \tag{13}$$

$$\bar p_1(\zeta,\xi) = -\bar u_1(\zeta,\xi) \tag{14}$$

where P denotes the Cauchy principal value of the integral. Here, $\bar v_1 = -\partial\bar\psi_1/\partial\zeta$ and $\bar u_1 = \partial\bar\psi_1/\partial\xi$. The $\bar v_1(\zeta,0)$ can be obtained from the zeroth-order boundary-layer equations. Introducing the expansions [Eq. (9)] into the boundary-layer equations (3–5), we obtain the following sets of equations:

$$\mathfrak{L}_0(1,\partial f_0/\partial\eta) = 0 \tag{15}$$

$$\mathfrak{L}_0(Pr,\theta_0) = -2Q\zeta y_{F0}^2 \exp(-\theta_\alpha/\theta_0) \tag{16}$$

$$\mathfrak{L}_0(Sc_F, y_{F0}) = 2\zeta y_{F0}^2 \exp(-\theta_\alpha/\theta_0) \tag{17}$$

$$\mathfrak{L}_0(1,\partial f_1/\partial\eta) = -f_1\ \partial^2 f_0/\partial\eta^2 + 2\zeta\{\partial f_1/\partial\eta\ \partial^2 f_0/\partial\eta\,\partial\zeta - \partial f_1/\partial\zeta\ \partial^2 f_0/\partial\eta^2 + \theta_0\ \partial p_0/\partial\zeta\} \tag{18}$$

$$\mathcal{L}_0(Pr,\theta_1) = -f_1\,\partial\theta_0/\partial\eta + 2\zeta\{\partial f_1/\partial\eta\,\partial\theta_0/\partial\zeta - \partial f_1/\partial\zeta\,\partial\theta_0/\partial\eta$$
$$- Q(2y_{F1}/y_{F0} + \theta_\alpha\theta_1/\theta_0^2)y_{F0}^2\exp(-\theta_\alpha/\theta_0)\} \tag{19}$$

$$\mathcal{L}_0(Sc_F,y_{F1}) = -f_1\,\partial y_{F0}/\partial\eta + 2\zeta\{\partial f_1/\partial\eta\,\partial y_{F0}/\partial\zeta$$
$$- \partial f_1/\partial\zeta\,\partial y_{F0}/\partial\eta + (2y_{F1}/y_{F0} + \theta_\alpha\theta_1/\theta_0^2)y_{F0}^2\exp(-\theta_\alpha/\theta_0)\} \tag{20}$$

with the boundary conditions given by

$$\text{at } \eta = 0, \qquad \zeta<\zeta_L:$$
$$f_0 = f_1 = \theta_1 = \partial f_0/\partial\eta = \partial f_1/\partial\eta = \partial y_{F0}/\partial\eta = \partial y_{F1}/\partial\eta = 0,$$
$$\theta_0 = \theta_w$$
$$\zeta>\zeta_L: f_0 = f_1 = \partial\theta_0/\partial\eta = \partial\theta_1/\partial\eta = \partial^2 f_0/\partial\eta^2 = \partial^2 f_1/\partial\eta^2$$
$$= \partial y_{F0}/\partial\eta = \partial y_{F1}/\partial\eta = 0$$
$$\text{for } \eta\to\infty: \partial f_0/\partial\eta\to 1, \qquad p_0 = \bar{p}_0 = 0,$$
$$\theta_0\to 1, \qquad y_{F0}\to 1, \qquad V_0\to\bar{v}_1(\zeta,0)$$
$$\partial f_1/\partial\eta\to\bar{u}_1(\zeta,0), \qquad p_1\to\bar{p}_1(\zeta,0), \qquad \theta_1 = y_{F1} = 0$$

where $\bar{u}_1(\zeta,0)$ and $\bar{p}_1(\zeta,0)$ must be obtained by solving the Cauchy integral [Eq. (13)], with the aid of the matching condition

$$V_0(\zeta,\eta\to\infty)\to\bar{v}_1(\zeta,\xi\to 0) \tag{21}$$

where V_0 is the transversal velocity in the boundary layer given as

$$V_0 = (2\zeta)^{-1/2}\{-f - 2\zeta\,\partial f/\partial\zeta + \eta\,\partial f/\partial\eta\}$$
$$- \partial f/\partial\eta\,\partial\int_0^{y^*}[(\rho^*/\rho_{00}^*)\,\mathrm{d}y^*]/\partial x^* \tag{22}$$

Therefore, since $\eta\to\infty$, V_0 behaves as

$$V_0\to(2\zeta)^{-1/2}\left\{C_0(\zeta) + 2\zeta\,\mathrm{d}C_0/\mathrm{d}\zeta + \lim_{\eta\to\infty}\left[\int_0^{\eta}\theta\,\mathrm{d}\eta' - \eta'\right]\right\} \tag{23}$$

where

$$C_0(\zeta) = \lim_{\eta\to\infty}\{\eta - f_0(\zeta,\eta)\} \tag{24}$$

The first two terms on the right-hand side of Eq. (23) take into account the momentum effects on the displacement thickness, and the third term is due to the very strong expansion effects.

The conditions close to the leading edge of the plate can be obtained in the limit $\zeta\to 0$. The momentum equation is the well-known Blasius equation

$$\mathrm{d}^3 f_0/\mathrm{d}\eta^3 + f_0\,\mathrm{d}^2 f_0/\mathrm{d}\eta^2 = 0 \tag{25}$$

together with the energy equation

$$\mathrm{d}^2\theta_0/\mathrm{d}\eta^2 + f_0 Pr\,\mathrm{d}\theta_0/\mathrm{d}\eta = 0 \tag{26}$$

For the specific case of $Pr = 1$, the nondimensional transversal velocity at the edge of the boundary layer is given by

$$V_0(\zeta\to 0,\eta\to\infty)\to(2\zeta)^{-1/2}\{1.216786\theta_w\} \tag{27}$$

In the case of frozen flow (no chemical reaction), the nondimensional normal velocity at the edge of the boundary layer given by Eq. (27) is obtained throughout the flowfield. Using the matching conditions given by Eq. (21), and solving the Cauchy integral [Eq. (13)], we obtain no pressure gradients in these first-order equations. However, as the combustion process takes place, the strong expansion of the gases displaces the outer potential flow in such a way that important pressure gradients are generated, affecting the flowfield upstream of the flame-formation position and showing the first appearance of a feedback mechanism.

Results and Discussion

The system of Eqs. (13-20) with the appropriate boundary and matching conditions was solved numerically using the multiple shooting technique. The boundary-layer (inner) equations are of the parabolic type; thus, marching in the ζ coordinate, together with shooting methods for the η coordinate, are employed to solve the equations. The first-order outer equation, given by the Cauchy integral [Eq. (13)] is then solved using the technique described elsewhere.[11] The pressure gradients obtained in this order are considered in the first-order inner boundary-layer equations. The numerical calculations were made for a stoichiometric mixture of propane and air[13] for different values of the wall temperature. Two general cases were considered. In the first case, the length of the plate is not enough to ignite the premixed gases. The flame is generated in the laminar wake of the plate. In the second case, we consider an infinite flat plate, that is, $\zeta_L\to\infty$. Here the flame is generated above the flat plate. Figure 1 shows a schematic diagram of the two cases considered. Figures 2-6 show the results obtained after numerical integration of both the zeroth- and first-order boundary-layer equations for the infinitely long plate. Two different values of the nondimensional wall tem-

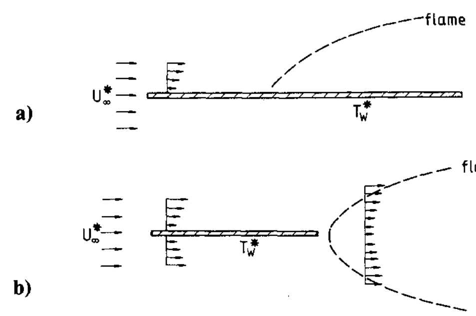

Fig. 1 Schematic diagram of the two cases considered: a) infinite flat plate; b) flame generated in the laminar wake of the flat plate.

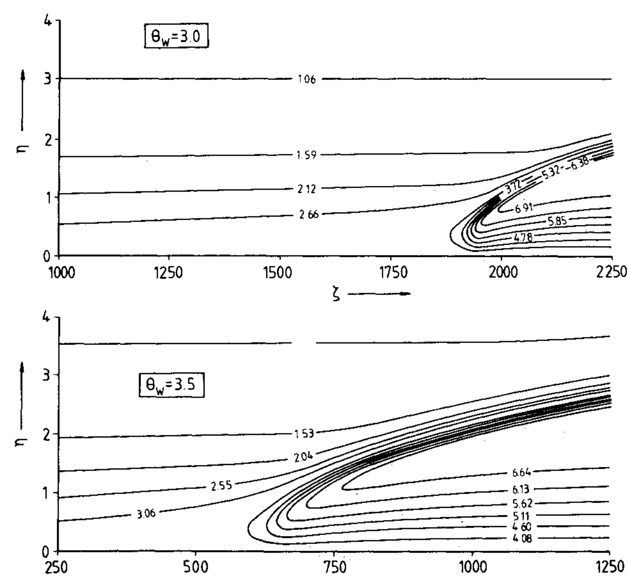

Fig. 2 Flame generated above the flat plate. Zeroth-order solution. Lines of θ_0 constant.

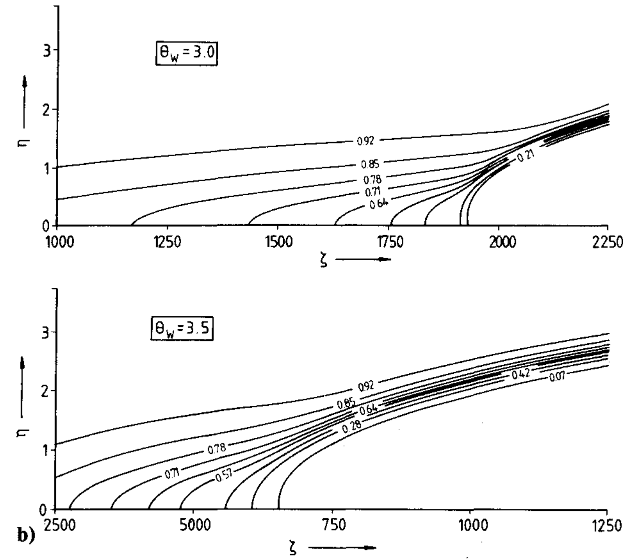

Fig. 3 Flame generated above the flat plate. Zeroth-order solution. Lines of y_{F0} constant.

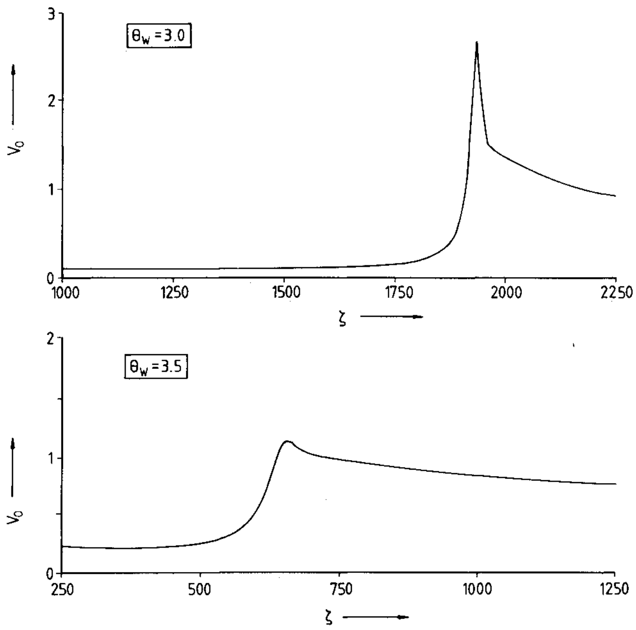

Fig. 4 Flame generated above the flat plate. Zeroth-order solution. Nondimensional transversal velocity component at the edge of the boundary layer $V_0(\eta\rightarrow\infty)$.

perature were assumed: $\theta_w = 3$ and 3.5. These values were chosen in order to evaluate the effect of the overall activation energy of the chemical reaction, through the Zeldovich number Z, defined as the ratio of the activation energy to the thermal energy $Z = \theta_a/\theta_w$.

Figures 2 and 3 show the zeroth-order temperature and fuel concentration profiles, respectively, for the two values of the nondimensional plate temperature. These figures clearly show the premixed flame formed above the flat plate. As the plate temperature decreases, the flame position moves away from the leading edge and generates larger longitudinal gradients in regions close to the flame leading edge.

Figures 4 shows the nondimensional normal velocity component at the edge of the boundary layer $V_0(\eta\rightarrow\infty)$. Because of the very strong expansion effects, this velocity peaks in regions close to the flame formation point. The peak amplitude is larger for larger values of the Zeldovich numbers. The corresponding first-order pressure distribution is shown in Fig. 5. The pressure also peaks in regions close to the flame

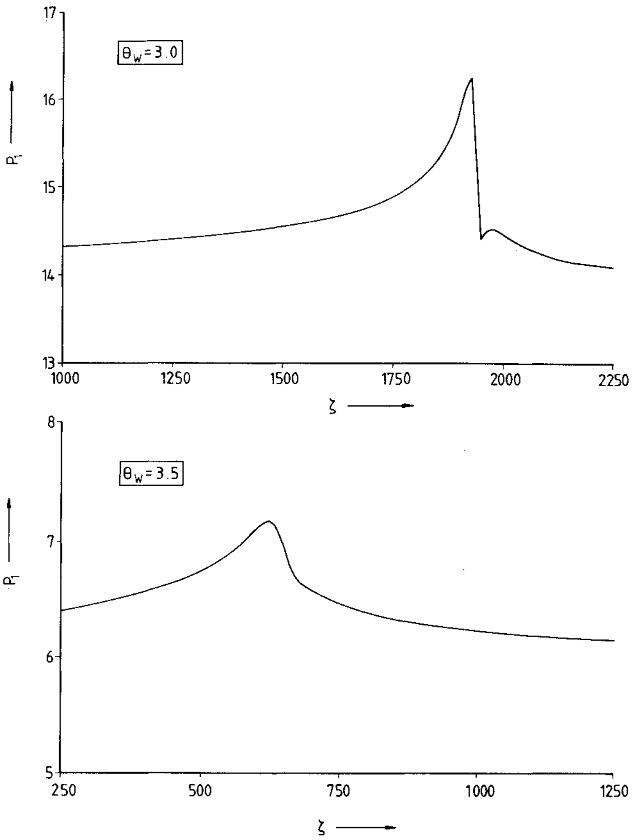

Fig. 5 Flame generated above the flat plate. First-order solution. Nondimensional pressure distribution.

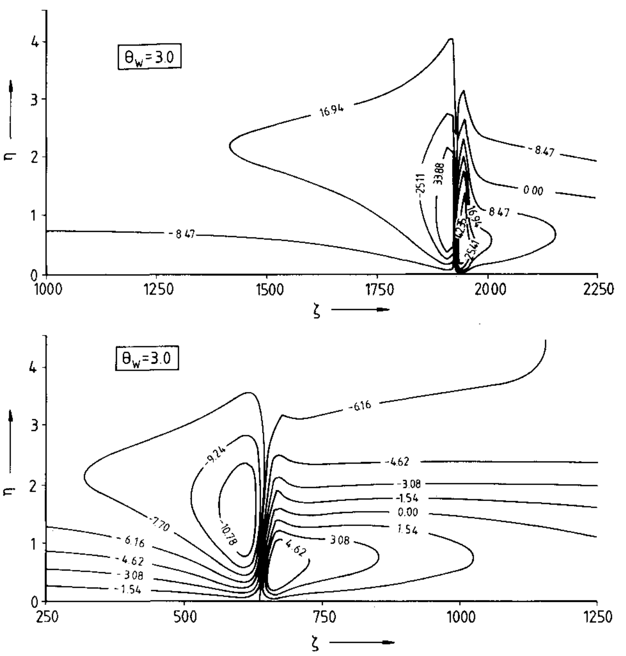

Fig. 6 Flame generated above the flat plate. First-order solution. Lines of u_1 constant.

leading edge. The expansion process produced by the exothermic reaction generates positive pressure in front of the flame-formation point and negative pressure gradients behind it. The induced first-order nondimensional axial velocity is shown in Fig. 6. Here we can observe that a low-velocity region is formed in front of the flame as a result of the positive pressure gradients. On the other hand, a high-velocity region is located behind this position. The intensity of these high- and low-velocity regions increases as the Zeldovich number increases.

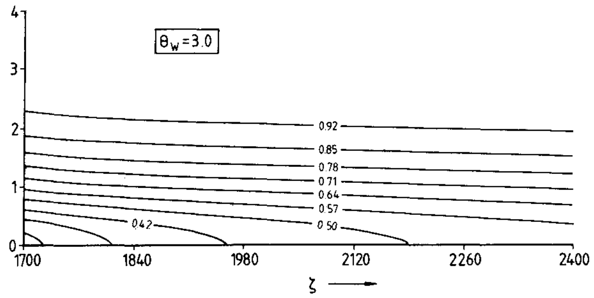

Fig. 7 Flame generated in the wake $\theta_w = 3$. Zeroth-order solution. Lines of u_0 constant.

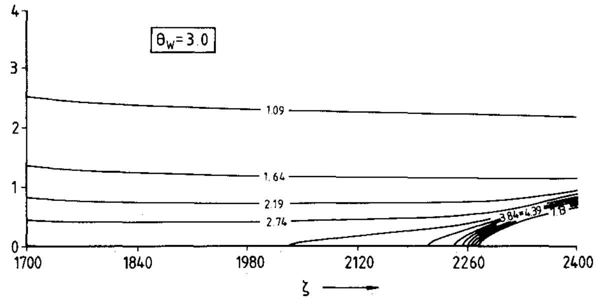

Fig. 8 Flame generated in the wake $\theta_w = 3$. Zeroth-order solution. Lines of θ_0 constant.

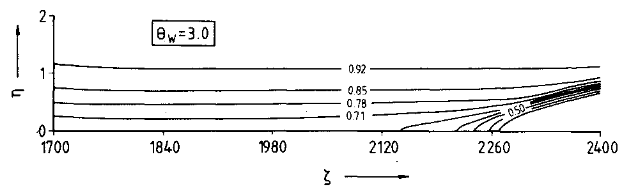

Fig. 9 Flame generated in the wake $\theta_w = 3$. Zeroth-order solution. Lines of y_{F0} constant.

Figures 7-12 show the results obtained after numerical integration of the zeroth- and first-order boundary-layer equations for the finite-length case. Here a heated plate $(0 \leq \zeta \leq 1638)$ is maintained at a constant nondimensional temperature $\theta_w = 3$. This relatively low temperature of the plate is sufficient to cause self-ignition in the wake behind the flat plate such that a premixed combustion zone is formed that in turn affects the structure of the flow. The singularity arising at the end of the plate[7,9] is assumed to have no influence in the region of interest. Therefore, the flow structure approaches the Goldstein wake type.[14] Figure 7 shows the zeroth-order nondimensional longitudinal fluid velocity. Here only the interesting part of the wake is shown $(\zeta > 1700)$. The expansion effects are included in the definition of the similarity coordinate η in this case. The nondimensional velocity at the centerline (behind the plate) increases, asymptotically reaching the value of unity as $\zeta \rightarrow \infty$.

Figures 8 and 9 show the profiles of the nondimensional temperature θ_0 and reactant concentration y_{F0}, respectively. These figures show how the premixed combustion zone is formed in the laminar wake of the flat plate. The nondimensional transversal velocity component V_0 at the edge of the boundary layer is shown in Fig. 10. This velocity distribution has been obtained from the solution of the zeroth- or leading-order boundary-layer equations. Because of the very strong thermal expansion effects, the velocity increases drastically in the combustion zone at the wake.

This abrupt change in the boundary-layer thickness displaces the outer inviscid flow, generating a pressure distribution shown in Fig. 11. The boundary-layer flow first generates a positive pressure gradient in the axial direction that ends at the region of self-ignition. Because of the curvature effects behind this zone, a negative pressure gradient is generated, causing the pressure to asymptotically reach the freestream pressure. The pressure gradients generated in the interaction with the outer inviscid flow affect the axial velocity component in an important way. In front of the combustion zone a low axial velocity region is formed as a result of the positive pressure gradient. Downstream, the negative pressure gradient generates a region of high axial velocity, which can provoke overshoot. The first-order axial nondimensional velocity pro-

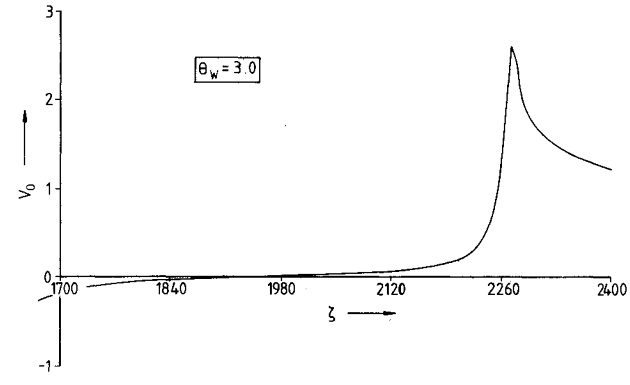

Fig. 10 Flame generated in the wake $\theta_w = 3$. Zeroth-order solution. Nondimensional transversal velocity component at the edge of the boundary layer $V_0(\eta \rightarrow \infty)$.

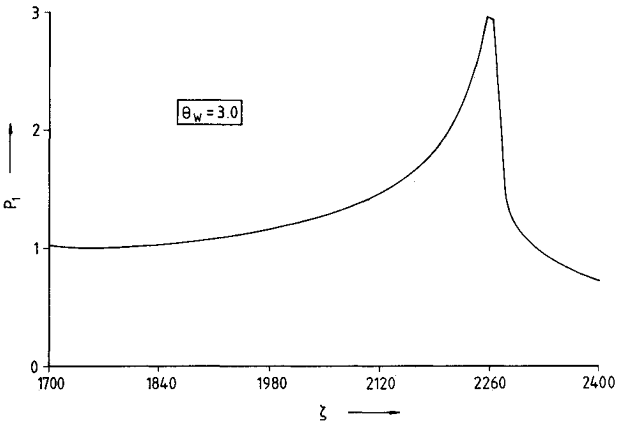

Fig. 11 Flame generated in the wake $\theta_w = 3$. First-order solution. Nondimensional pressure distribution.

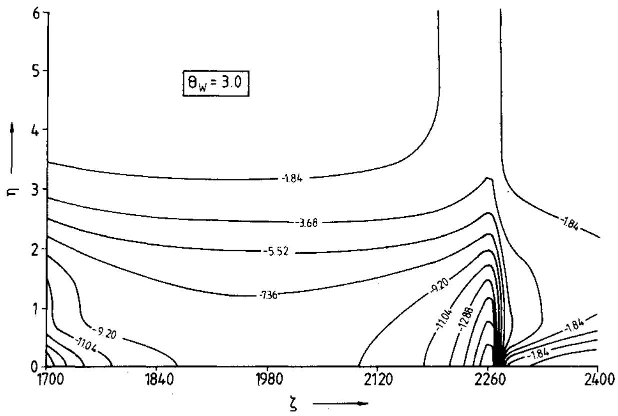

Fig. 12 Flame generated in the wake $\theta_w = 3$. First-order solution. Lines of u_1 constant.

files are shown in Fig. 12. The low- and high-velocity regions are close to each other in the flame-formation region.

Conclusions

An asymptotic analysis has been performed so that the higher-order effects in the premixed combustion in a boundary-layer flow could be studied using the inverse of the square root of the Reynolds number as the small parameter of expansion. The zeroth-order solution corresponds to the Prandtl boundary-layer approximation. The first-order solution takes into account the interaction with the inviscid flow. This interaction makes it possible to introduce a feedback mechanism through the generation of pressure gradients. A positive pressure gradient is induced in front of the flame leading edge, thus producing a low-velocity region. The intensity of these pressure gradients strongly depends on the Zeldovich numbers. This interaction caused by the strong expansion effects in boundary-layer combustion is always important and must be taken into account in this type of flow.

Acknowledgments

This work has been sponsored by the Volkswagen-Stiftung of the Federal Republic of Germany. C. Treviño also acknowledges the support of the Alexander von Humboldt Stiftung during his stay in Aachen.

References

[1]Turcotte, D. L., "Stable Combustion of a High Velocity Gas in a Heated Boundary Layer," *Journal of the Aeronautical Sciences,* Vol. 27, 1960, pp. 509-516.

[2]Toong, T. Y., "Ignition and Combustion in a Laminar Boundary Layer Over a Hot Surface," *6th International Symposium on Combustion,* Reinhold, New York, 1957, pp. 532-540.

[3]Toong, T. Y, "Flame Stabilization in Boundary Layers," *Combustion and Propulsion,* AGARD III Colloquium, Pergamon, New York, 1958, pp. 581-597.

[4]Hirano, T. and Kanno, Y. "Aerodynamical and Thermal Structures of a Laminar Boundary Layer Over a Flat Plate With a Diffusion Flame," *14th Symposium (International) on Combustion,* The Combustion Inst., Pittsburgh, PA, 1973, p. 391.

[5]Kuo, Y. H., "On the Flow of an Incompressible Viscous Past a Flat Plate at Moderate Reynolds Numbers," *Journal of Mathematical Physics,* Vol. 32, 1953, pp. 83-101.

[6]Imai, I., "Second Approximation to the Laminar Boundary Layer Flow Over a Flat Plate," *Journal of the Aeronautical Sciences,* Vol. 24, 1957, pp. 155-156.

[7]Stewardson, K., "Multistructured Boundary Layers on Flat Plates and Related Bodies," *Mathematika,* Vol. 16, 1969, pp. 146-239.

[8]Messiter, A. F., "Boundary Layer Flow Near a Trailing Edge of a Flat Plate," *SIAM Journal of Applied Mathematics,* Vol. 18, 1970, pp. 241-257.

[9]Messiter, A. F. and Liñán, A., *Zeitschrift fuer Angewandte Mathematik und Physik,* Vol. 27, 1976, p. 634.

[10]Treviño, G. and Fernández-Pello, A. C., "Aerodynamics of Premixed Flames in Flat Plate Boundary Layers," *Combustion Science and Technology,* Vol. 38, 1984, pp. 293-312.

[11]Treviño, C., Stüttgen, W., and Peters, N., "Pressure Gradients Due to Gas Expansion and Gasification Effects in a Boundary Layer Combustion of a Condensed Fuel," *Waerme und Stoffuebertragung,* 1989 (to be published).

[12]Lighthill, M. J., "A New Approach to Thin Airfold Theory," *Aeronautical Quarterly,* Vol. 3, 1951, pp. 193-210.

[13]Sharma, O. P. and Sirignano, W. A., "On the Ignition of a Premixed Fuel by a Hot Projectile," *Combustion Science and Technology,* Vol. 1, 1970, pp. 481-494.

[14]Goldstein, S., "On the Two-Dimensional Steady Flow of a Viscous Fluid Behind a Solid Body," *Proceedings of the Royal Society of London, Series A,* Vol. 142, 1933, pp. 545-562.